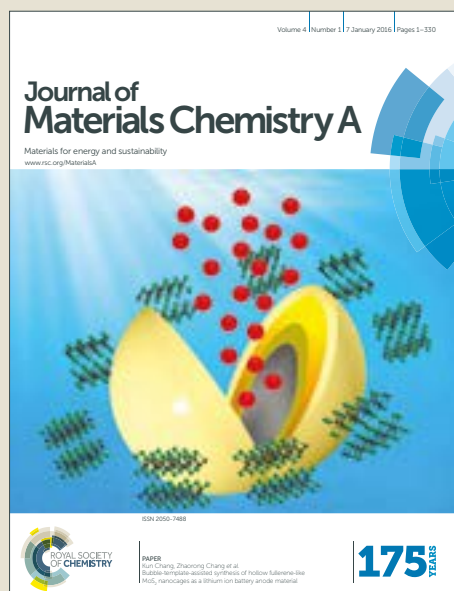


Journal of Materials Chemistry A

Accepted Manuscript



This article can be cited before page numbers have been issued, to do this please use: J. Gandara-Loe, A. Missyul, F. Fauth, L. L. Daemen, Y. Cheng, A. J. Ramirez-Cuesta, P. Ravikovitch and J. Silvestre-Albero, *J. Mater. Chem. A*, 2019, DOI: 10.1039/C8TA09713E.



This is an Accepted Manuscript, which has been through the Royal Society of Chemistry peer review process and has been accepted for publication.

Accepted Manuscripts are published online shortly after acceptance, before technical editing, formatting and proof reading. Using this free service, authors can make their results available to the community, in citable form, before we publish the edited article. We will replace this Accepted Manuscript with the edited and formatted Advance Article as soon as it is available.

You can find more information about Accepted Manuscripts in the [author guidelines](#).

Please note that technical editing may introduce minor changes to the text and/or graphics, which may alter content. The journal's standard [Terms & Conditions](#) and the ethical guidelines, outlined in our [author and reviewer resource centre](#), still apply. In no event shall the Royal Society of Chemistry be held responsible for any errors or omissions in this Accepted Manuscript or any consequences arising from the use of any information it contains.

New insights into the breathing phenomenon in ZIF-4

Jesus Gandara-Loe,^a Alexander Missyul,^b François Fauth,^b Luke L. Daemen,^c Yongqiang Q. Cheng,^c Anibal J. Ramirez-Cuesta,^c Peter I. Ravikovitch,^d and Joaquin Silvestre-Albero^{*,a}

Received 00th January 20xx,
Accepted 00th January 20xx

DOI: 10.1039/x0xx00000x

www.rsc.org/

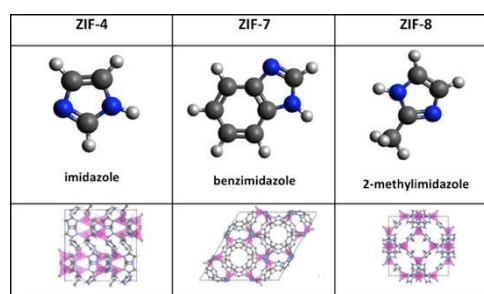
Structural changes in ZIFs upon adsorption remain a paradigm due to the sensitivity of the adsorption mechanism to the nature of the organic ligands and gas probe molecules. Synchrotron X-ray diffraction under operando conditions clearly anticipate for the first time that ZIF-4 exhibits a structural reorientation from a narrow-pore (np) to a new expanded-pore (ep) structure upon N₂ adsorption, while it does not for CO₂ adsorption. The existence of an expanded-pore structure of ZIF-4 has also been predicted by molecular simulations. In simulations the expanded structure was stabilized by entropy at high temperatures, and by strong adsorption of N₂ at low temperatures. These results are in perfect agreement with manometric adsorption measurements for N₂ at 77K that show the threshold pressure for the breathing at ~30 kPa. Inelastic neutron scattering (INS) measurements show that CO₂ is also able to promote structural changes but, in this specific case, only at cryogenic temperatures (5K).

Introduction

Zeolitic-imidazolate frameworks (ZIFs) is a new subfamily of the metal-organic frameworks (MOFs). These structures consist in metallic centers in a tetrahedral coordination (MN₄) linked through imidazolate linkers, the final topology being rather similar to those observed in zeolites (for instance the M-Im-M bond resembles that in zeolites Si-O-Si, i.e. 145⁹).¹⁻³ One of the most important characteristics of this group of materials is the presence of structural changes/transformations upon an external stimuli (for instance upon gas adsorption, a heat treatment or under high-pressure conditions). Interestingly, the nature of these phenomena highly depends on the kind of functionality present in the imidazolate linker (scheme 1). Indeed, the nature of the functional group defines the competition within the ZIF structure between strong non-bonding interactions (van der Waals and electrostatic), which favor the formation of highly dense structures (e.g. desolvated ZIF-7), and bonding interactions (mainly torsional and bending), that favors the formation of high symmetry, low-density crystal structure.

For instance, in the specific case of the methyl-based imidazolate, the one present in ZIF-8, previous studies described in the literature have shown that this material exhibits a gate-opening phenomenon upon an external pressure or upon gas adsorption (above ~2 kPa in the specific case of N₂).^{4,5} This gate-opening is associated with the

swinging of the imidazolate linkers above a given threshold pressure, and depends on the nature of the probe molecule.⁶ On the contrary, a closely related ZIF with the same SOD topology, sharing the same metal atoms (Zn), the only difference being the nature of the ligand, i.e. benzimidazolate in the specific case of ZIF-7, gives rise to a completely different scenario. Recent studies described in the literature have shown that upon gas adsorption there are associated phase-to-phase transitions, the threshold pressure for these changes being also sensitive to the nature of the adsorptive molecule. Experimental results and mathematical modeling clearly anticipate a breathing effect from a narrow-pore highly dense structure, phase I, to a large-pore low-density framework, phase II.^{7,8}



Scheme 1. Molecular structure of the organic linker and 3D structure of some ZIFs with structural flexibility.³

As described above, the core structure of these fascinating ZIFs is a network of Zn metallic centers tetrahedrally coordinated through substituted imidazolate linkers. The most basic of these structures, i.e. the one constituted by un-substituted imidazolate linker, corresponds to ZIF-4. This ZIF has an orthorhombic space group with *cag* network topology of the mineral variscite and pore size windows of 0.21 nm in diameter.⁹ Recent studies have shown that despite the

^a Laboratorio de Materiales Avanzados, Departamento de Química Inorgánica-IUMA, Universidad de Alicante, E-03690 San Vicente del Raspeig, Spain. *Email - joaquin.silvestre@ua.es

^b CELLS-ALBA Synchrotron, E-08290 Cerdanyola del Vallés, Spain.

^c Oak Ridge National Laboratory, Spallation Neutron Source, 1 Bethel Valley Road, Oak Ridge, TN 37831, USA.

^d ExxonMobil Research and Engineering Co., Annandale, New Jersey, 08801, USA.

†Electronic Supplementary Information (ESI) available: [Complete characterization of ZIF-4 nanocrystals, CO₂ adsorption isotherms, synchrotron XRD patterns after CO₂ adsorption, inelastic neutron scattering measurements and molecular simulations]. See DOI: 10.1039/x0xx00000x

small pore window predicted theoretically, ZIF-4 is indeed able to adsorb N_2 and even small hydrocarbons.^{9,10} N_2 adsorption measurements described by Bennett et al. anticipate structural changes upon N_2 adsorption, although the reason behind these phenomena have never been evaluated. Despite the importance of this specific ZIF to get a better understanding of this sub-class of materials and their associated structural transformation, the number of studies reported in the literature is rather scarce.^{2,9-12}

With this in mind, the aim of this study is to ascertain the nature of these structural changes in ZIF-4 upon gas adsorption by combining synchrotron X-ray diffraction and inelastic neutron scattering studies under *operando* conditions, and molecular simulation studies.

Results and discussion

The details about the synthesis and the main characteristics of the synthesized ZIF-4 nanocrystals can be found in the supporting information (Fig. S1 and S2). Fig. 1 reports the N_2 adsorption/desorption isotherm for ZIF-4 at cryogenic temperatures, including the kinetic data for each physisorption point.

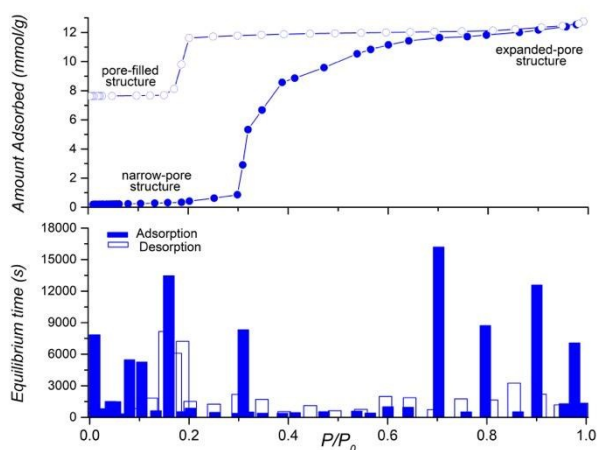


Fig. 1. N_2 adsorption (filled symbols)/desorption (empty symbols) isotherm for ZIF-4 at 77K (upper panel). Time requested to reach equilibrium for each of the adsorption and desorption points (lower panel).

The amount of nitrogen adsorbed below 0.4 relative pressure is rather small due to the inaccessibility of the nitrogen molecules to the inner porous structure. However, above a certain threshold pressure, i.e. above 30 kPa, the nitrogen adsorption capacity experiences a sudden increase in the amount adsorbed up to a maximum of *ca.* 12.5 mmol g^{-1} (or 280 $\text{cm}^3 \text{STP g}^{-1}$) at 103 kPa. Upon desorption the material remains unaltered, i.e. nitrogen is kept entrapped in the inner porosity down to a given pressure, *ca.* 21 kPa, when the material suddenly desorbs partially these nitrogen molecules down to a constant value of $\sim 7.6 \text{ mmol g}^{-1}$. The shape of the isotherm and the breathing phenomenon at medium pressures is in close agreement with the N_2 isotherm reported in the literature by Bennett et al. for ZIF-4.⁹ At this point it is important to emphasize that contrary to some assumptions reported in the literature, ZIF-4 isotherm does not allow to estimate the monolayer capacity using the BET equation (due to the absence of nitrogen adsorption in the

relative pressure range 0-0.3) and consequently, to estimate the apparent surface area.

DOI: 10.1039/C8TA09713E

Taking a closer look to the decay in the manifold pressure versus time to reach equilibrium for each of the adsorption/desorption points in the N_2 isotherm (kinetic data), Fig. 1 (lower panel) clearly shows that the adsorption behavior in ZIF-4 is rather complex compared to conventional nanoporous solids. Before the breathing or opening of the structure, adsorption points are extremely slow at specific pressures. Once the threshold pressure of $\sim 30 \text{ kPa}$ has been reached, the structure opens and kinetics are faster up to $\sim 73 \text{ kPa}$. Above this pressure, a further expansion of the unit cell is associated with slow kinetics, but only in alternating adsorption points. This sawtooth-like adsorption performance is quite unique and it is associated with the necessity to break down intermolecular interactions to open-up the porous structure through the crystals. Compared to previous studies with analogues ZIF-8 and ZIF-7, the breathing behavior in ZIF-4 takes place at a much higher relative pressure, i.e. $\approx 2 \text{ kPa}$ for ZIF-8 and $\approx 3.3 \text{ kPa}$ for ZIF-7.^{4,8} This observation anticipates the presence of stronger non-bonding interactions in the ZIF-4 with un-substituted linker that inhibits the expansion of the porous network.

To gain more knowledge about the breathing phenomenon in ZIF-4, synchrotron X-ray powder diffraction (SXPDP) studies were performed at the MSPD station in ALBA synchrotron (Spain). Desolvated ZIF-4 was cooled down to 80 K under vacuum and N_2 doses were incorporated in the capillary cell up to atmospheric pressure followed by an evacuation step, trying to reproduce the adsorption measurements described above. Fig. 2 shows the SXPDP pattern corresponding to ZIF-4 under *operando* conditions. Variations in the unit cell parameters were analyzed by Le Bail fitting. The Rietveld refinement of the desolvated sample at 298 K (Figure S1) confirms that its crystal structure corresponds to ZIF-4 without observable amount of impurities.¹¹ Lattice parameters are $a = 15.4936(7) \text{ \AA}$, $b = 15.5110(7) \text{ \AA}$, $c = 18.0468(8) \text{ \AA}$ ($V = 4337.0(5) \text{ \AA}^3$). Afterwards the ZIF-4 sample was cooled down under vacuum to 80 K before the incorporation of N_2 . At cryogenic temperatures the unit cell parameters exhibit a small contraction (1%), so that the new lattice parameters at 80 K are $a = 15.507(5) \text{ \AA}$, $b = 15.098(2) \text{ \AA}$, $c = 18.354(4) \text{ \AA}$ ($V = 4297(2) \text{ \AA}^3$). The small contraction in the unit cell at 80 K differs from the values previously reported so far by Wharmby et al., where a porous to dense phase transition with up to 23% contraction in the unit cell was observed at 80 K ($V = 3344.77(4) \text{ \AA}^3$).¹¹ These authors observed that this contraction is indeed crystal-size dependent, i.e. larger crystals exhibit a smaller contraction. However, our experiments suggest that the value of 1% is quite reproducible independently of the crystal size evaluated. At this point it is important to highlight that we could observe a larger unit cell contraction when performing a fast cooling step, i.e. under non-equilibrium conditions.

As can be appreciated in Fig. 2, the SXPDP pattern of ZIF-4 does not exhibit any significant change after incorporation of 20 kPa of N_2 . However, incorporation of 40 kPa gives rise to important changes in the SXPDP pattern that evolve progressively until reaching 103 kPa, i.e. two different phases prevail until saturation. Upon N_2 dosing (only a few minutes were left after dosing N_2 and before recording the spectra) some peaks disappear (for instance 2.72° , 3.35° , 3.62° and 4.88°) and some new peaks emerge (3.55° , 3.80° and 4.72°), among others. These structural changes are associated with the

prevalence of two different phases, the low-temperature phase described above and a new phase characterized by a significant expansion in the unit cell parameters (up to 8-9% vol. expansion). The lattice parameters for the expanded-pore (N_2) ZIF-4 are $a = 15.960(3)\text{\AA}$, $b = 15.908(3)\text{\AA}$, $c = 18.311(3)\text{\AA}$ ($V = 4649(2)\text{\AA}^3$).

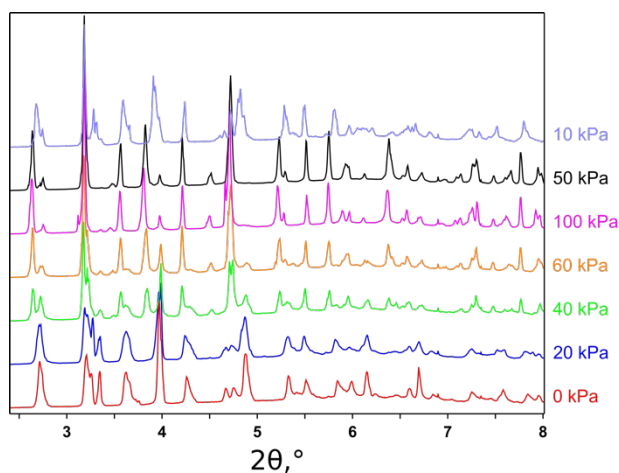


Fig. 2. Synchrotron X-ray diffraction pattern of ZIF-4 at 80 K after dosing N_2 (adsorption and desorption).

Fig. 3 shows the evaluation of the unit cell parameters for the ZIF-4 sample upon nitrogen adsorption obtained after Le Bail fitting. These results are perfectly coincident with the nitrogen adsorption measurements described above, i.e. below p/p_0 0.4 only the narrow-pore ZIF-4 structure is present. However, above this threshold pressure both phases (narrow-pore and expanded-pore) prevail up to atmospheric pressure when the expanded-pore (ep) structure is the only phase present. As described above, the unit cell expansion upon N_2 dosing is $\sim 8-9\%$ or $\Delta V = \sim 350\text{\AA}^3$. Taking into account the formula weight for ZIF-4 ($399.0374\text{ g mol}^{-1}$), this expansion corresponds to an increase of $\sim 0.53\text{ cm}^3\text{ g}^{-1}$. A closer look to Fig. 1 clearly shows that at atmospheric pressure ZIF-4 is able to adsorb 12.5 mmol g^{-1} or $0.44\text{ cm}^3\text{ g}^{-1}$ (as a liquid). The agreement between the adsorption experiments and the crystallographic measurements clearly confirms the validity and reproducibility of these measurements.

Upon expansion, the capillary was evacuated down to $\sim 50\text{ kPa}$. As observed in Fig. 2, the SPXRD pattern does not exhibit any change, in close agreement with the adsorption values. Only at $\sim 10\text{ kPa}$ the pattern exhibits important changes, the final pattern having certain similarities with the initial narrow-pore ZIF-4, although with possible symmetry lowering. According to these results, upon evacuation ZIF-4 exhibits a phase transition from an expanded-pore structure to a pore-filled structure trapping inside up to 7.6 mmol/g of nitrogen. The pore-filled structure has some similarities with the high-temperature (HT) structure reported in the literature for ZIF-4.¹¹ The structural parameters of the pore-filled structure are $a = 15.644(2)\text{\AA}$, $b = 15.140(2)\text{\AA}$, $c = 18.411(2)\text{\AA}$ ($V = 4361(1)\text{\AA}^3$). In summary, these results confirm for the first time the presence of two phase-to-phase transitions in ZIF-4, i) from narrow (np) to expanded-pore (ep) upon N_2 adsorption and ii) from expanded-pore (ep) to a pore-filled structure upon nitrogen evacuation at 77K.

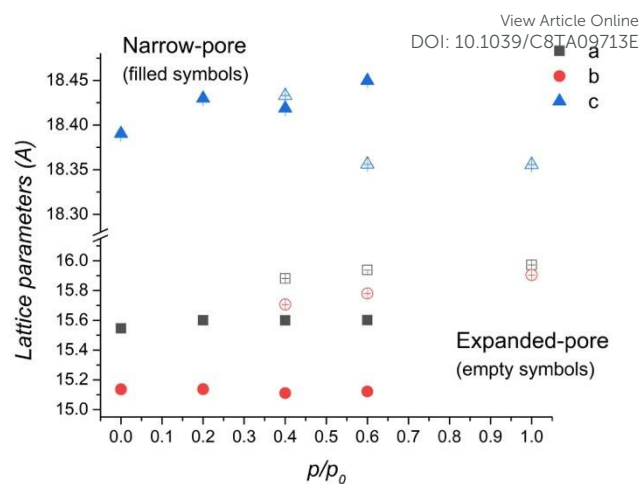


Fig. 3. Evolution of the unit cell parameters in ZIF-4 before and after dosing N_2 at 80K.

The existence of an expanded-pore structure of ZIF-4 has been predicted by classical Molecular Dynamics simulations (see Supporting Information for details). We followed the procedure and forcefield some of us used earlier to predict temperature-induced phase transition in ZIF-7.¹³ This forcefield reproduces well the structural properties of ZIFs, including unit cell constants, mechanical moduli (Table S6), and vibrational densities of states. In particular, it reproduces the low-frequency vibrational modes identified by INS (described later), e.g., the flapping of the imidazole ligand at $\sim 3\text{ meV}$ (Figure S3).

For the prediction of the pore-expanded ZIF-4 structure we used a series of NpT simulations with anisotropic barostat, and raised the temperature step-wise to gradually increase entropic contributions to the free energy ($F = E - TS$) and drive the system to an expanded phase with a larger entropy, and thus overall lower free energy. Figs. 4 and S4 show evolution of the unit cell parameters during MD simulations in comparison with experimental data for the reported low-temperature ZIF-4 transition¹¹ and for the pore expanded ZIF-4. The results in Fig. 5 demonstrate that an expanded-pore ZIF-4 is thermodynamically feasible upon heating despite having higher enthalpy. The resulting unit cell parameters $a = 15.8\text{\AA}$, $b = 16.1\text{\AA}$, $c = 18.9\text{\AA}$ ($V = 4799\text{\AA}^3$) are in very good agreement with the XRD measurements on the expanded-pore (N_2) ZIF-4 obtained experimentally. The predicted total pore volume of an expanded ZIF-4 ($V_p = 0.45\text{ cm}^3/\text{g}$) is also in good agreement with the N_2 adsorption measurements (Fig. 1), assuming the normal liquid density of N_2 in the pores. Moreover, we identify the second step on the desorption branch of N_2 isotherm with the transition back to a pore-filled ZIF-4 structure ($V_p = 0.24\text{ cm}^3/\text{g}$). The expanded ZIF-4 structure has significantly more open channels in the y-direction as compared to the reported ZIF-4 structure (Fig. 5).

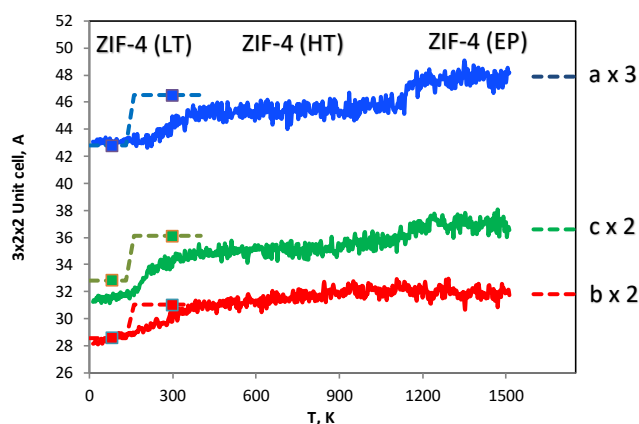


Fig. 4. Unit cell parameters from Molecular Dynamics simulation of the phase transitions in ZIF-4 upon heating. Shown are unit cell parameters for the 3x2x2 supercell. The narrow pore structure ZIF-4 (LT) transitions first into the open pore structure ZIF-4 (HT) at around 200-300 K, and then into expanded pore ZIF-4 (ep) structure. The dashed lines with points are experimentally measured unit cell parameters from Ref. [11]. The dashed lines on the right are the unit cell parameters experimentally measured in this work for the expanded pore ZIF-4 (ep) upon N₂ adsorption at 77 K.

We have also simulated expanded ZIF-4 structure with adsorbed N₂ molecules at 77 K at a loading of 10.3 mmol/g. We used Grand Canonical Monte Carlo (GCMC) simulations to load the structure with N₂ molecules, and performed NpT simulations (see Supporting Information for details), which confirmed stability of the pore-expanded ZIF-4 structure (Fig. S5). The resulting lattice parameters for the simulated (N₂) ZIF-4 $a = 15.7 \text{ \AA}$, $b = 16.0 \text{ \AA}$, $c = 18.6 \text{ \AA}$ ($V = 4655 \text{ \AA}^3$) are in even better agreement with the XRD measurements. Thus, interactions with N₂ also stabilized the expanded ZIF-4 structure even at low temperatures (Fig. S5). To prove that this is the case we performed NpT simulations at 77 K starting with an empty expanded ZIF-4 (ep) structure. During simulations it relaxed back to an intermediate structure ($V = 3587 \text{ \AA}^3$), which is in between reported ZIF-4 (HT) and ZIF-4 (LT) structures (Fig. S6). The existence of yet another ZIF-4 structure suggests a complex free-energy landscape, and agrees qualitatively with our cooling experiments, in which ZIF-4 (HT) did not fully contract to the previously reported ZIF-4 (LT) structure.

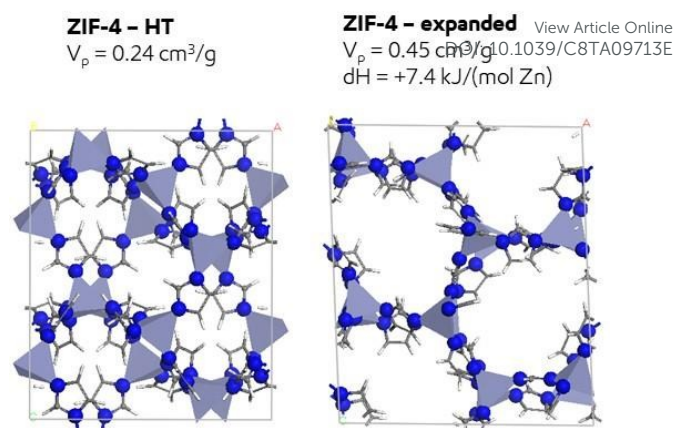


Fig. 5. Open ZIF-4 (HT) structure and predicted expanded-pore (ep) ZIF-4 structure. The enthalpy difference was obtained from MD simulations.

The adsorption performance of ZIF-4 has also been evaluated for CO₂ as a probe molecule at a much higher adsorption temperature. Fig. S8 shows the CO₂ adsorption isotherms at 273 K and up to 103 kPa. As can be appreciated, contrary to N₂, CO₂ is able to access the inner porous structure already at low relative pressures. The filling of the ZIF-4 cavities with CO₂ is relatively fast compared to N₂ (equilibrium time does not exceed 800 min, independently of the adsorption/desorption branch). The total amount adsorbed at atmospheric pressure is 3.2 mmol g⁻¹ at 273 K. Applying the Dubinin-Radushkevich (DR) equation to the CO₂ adsorption data gives rise to an accessible micropore volume of 0.21 cm³ g⁻¹ (CO₂ liquid density at 273 K is 1.023 g cm⁻³), quite far from the nitrogen adsorbed volume (i.e. 0.43 cm³ g⁻¹). Assuming the Gurvich rule for ZIF-4, the total amount of nitrogen and CO₂ adsorbed as a liquid would be the same, provided that both adsorbates are able to access the same porosity. However, the concave shape of the CO₂ isotherm and the faster kinetics do not anticipate any breathing, expansion or gate-opening phenomena. Taking into account that CO₂ is smaller than N₂ (0.33 nm vs. 0.36 nm) and the higher temperature of the adsorption measurement (298 K vs. 77 K), i.e. associated with faster kinetics, the lower adsorption capacity for CO₂ (3.2 mmol/g vs. 12.5 mmol/g) and the absence of a clear breathing phenomena anticipates that the expansion of the ZIF-4 structure upon gas adsorption is not a kinetic or steric effect but rather an energetic process. The absence of structural changes upon CO₂ adsorption has been corroborated by synchrotron powder X-ray diffraction measurements. According to Fig. S9, incorporation of CO₂ up to 103 kPa at 298 K and the corresponding desorption step does not produce significant changes in the SPXRD pattern.

Last but not least, the vibrational and rotation modes of ZIF-4 have been evaluated using inelastic neutron scattering measurements. These studies have been performed at the beamline VISION at the Oak Ridge National Laboratory (USA). INS is especially sensitive to the dynamics of hydrogen within a structural network due to the relatively large incoherent neutron cross-section of hydrogen compared to other atomic nuclei. Furthermore, due to the absence of selection rules, all transitions are active in INS, thus providing a

powerful tool to evaluate structural deformations in ZIFs.^{3,4,8} Fig. 6 shows the low energy transfer region for the ZIF-4 measured at 5 K and the simulated spectra obtained using VASP model. The theoretical results were then converted to the simulated INS spectra using the aClimax software.¹⁴ This low transfer energy region is the terahertz region and contains the most valuable information for ZIFs since it reveals dynamics of open and closed frameworks. The mid-high energy region (50-250 meV) contains the ring deformation modes and the C-C and C-H bending modes from the linker (see Supporting information). As it can be observed, the original sample exhibits a rather smooth spectra with a main contribution at 5.05 meV (40.7 cm⁻¹) and two small contributions at 6.90 meV (55.6 cm⁻¹) and 13.10 meV (105.6 cm⁻¹). Theoretical results clearly show that VASP allows for a good fitting of the experimental data, including the high energy modes (see Fig. S10), except the contribution at 5.05 meV. The higher neutron flux at VISION allows for a higher resolution of the INS spectra for ZIF-4, thus allowing for a better evaluation of the structural phenomena upon gas adsorption.³

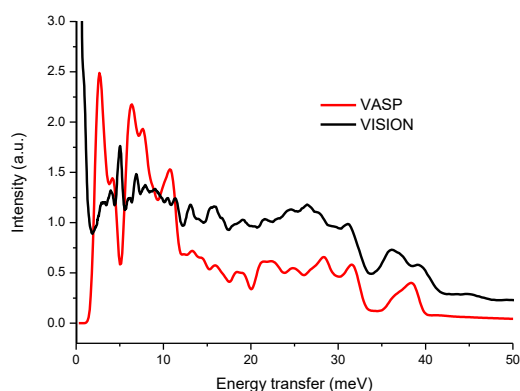


Fig. 6. INS spectra of ZIF-4 at 5 K compared with the simulated spectra using VASP model.

Theoretical predictions anticipate that all contributions below 40 meV are rather similar in nature and involve the libration/flapping of the imidazole ring. More specifically, within this range the lowest energies correspond to the rotation of the rings through the Zn-N axis (see animation in the SI), while higher energies involve the ring libration modes involving Zn-N stretch. The assignment of the low energy peaks (ca. 3-5 meV) to the ring rotation/flapping mode implies that these peaks will be highly affected by the compression/expansion of the unit cell upon an external stimuli (e.g. temperature and pressure change or upon adsorption). Indeed, this could be the reason to explain the differences between simulations and experiments, i.e. whereas simulations are performed using the structure at 80 K (LT structure), at the low temperature of the INS experiment (5 K) an additional unit cell contraction is expected, thus explaining the appearance of this additional peak at 5 meV, not predicted by the models. Classical molecular simulations (Fig. S3) also does not predict the 5 meV peak.

It is reasonable to assume that in the contracted structure the flapping of the imidazole ligand, theoretically predicted at 3 meV, will be hindered and shifted to a slightly higher energy value (ca. 5.05

meV). Incorporation of 103 kPa of nitrogen to ZIF-4 at 80 K and subsequent cooling down to 5 K gives rise to the same INS spectra (see Fig. S11). Although this observation is in contradiction with the synchrotron X-ray diffraction measurements, it must be attributed to the instability of N₂ in the cavities of the ZIF-4 at extremely low temperatures (i.e. 5 K). Indeed, a similar instability of N₂ was reported for ZIF-7 upon slight variations in temperature around 80 K.⁸ On the contrary, incorporation of 103 kPa of CO₂ at 298 K and further cooling down to 5 K gives rise to interesting findings. Under these conditions the suppression of the contribution at 5.05 meV can be clearly appreciated (see Fig. S12). Taking into account that the spectra of ZIF-4 filled with CO₂ resembles that predicted by the model at 298 K, this could be an indication of the filling of the cavities by CO₂ at these extremely low temperatures, so that the adsorption of CO₂ produces a structural change, probably from the narrow-pore (*np*) to the certain expanded-pore (*ep*) structure.

It should be noted that at least two other publications indirectly confirm the existence of the pore-expanded ZIF-4. In the work of Bennet et al⁹ the measured N₂ adsorption isotherms agree almost perfectly with our isotherm in Fig. 1, thus confirming the validity of our experiments. Recently Hwang et al¹⁵ found an unusual dependence for diffusivities of alkanes in ZIF-4. They hypothesized that the structure can expand upon adsorption of pentane. Our experimental and modeling results strongly suggest that this indeed could be the case, and that other molecules can cause transition to the expanded-pore ZIF-4 (*ep*). We performed GCMC simulations with the pore-expanded structure and were able to match the maximum experimental loading of pentane of 2.5 mmol/g (Figure S7).

Experimental

Synthesis of ZIF-4

ZIF-4 crystal were synthesized following the recipe described by Yaghi et al. with some modifications.² In an initial step, a solid mixture of 0.4 g Zn(NO₃)·4H₂O and 0.3 g imidazole was prepared in a 100 ml beaker. Afterwards, 30 ml of N,N-dimethylformamide were added drop wise and the solution was ultrasonicated for 30 min. After ultrasonication, the beaker containing the solution was sealed with silicon stopper and heated to 403 K (heating ramp 5 K/min) for 48h. Since the control of the temperature is crucial to get high-quality crystals, sand-bath was used to control the temperature. Once the thermal treatment is done, the mixture must be cooled down to room temperature very slowly and left for additional 96h at 268 K in the fridge. At the end, large colorless rhombohedral ZIF-4 crystals are obtained (see Figure S2). These crystals must be washed with 30 ml DMF (x2) and methanol (x2). Finally the crystals are dried at 323 K for 1h. At this point it is important to highlight the necessity of the step at 268 K for 96h to allow time for the growth of micron-size ZIF-4 crystals. If this step is not performed properly, a white powder is obtained with mixtures of nano-crystalline ZIF-4 and an "unknown" phase.

Characterization of the synthesized ZIF-4

Synthesized ZIF-4 crystals have been evaluated using a number of techniques. Textural properties have been evaluated using N₂ adsorption/desorption measurements at cryogenic temperatures.

Before the adsorption experiment, ZIF-4 crystals were outgassed at 413 K for 48h under high vacuum (10^{-7} kPa). Nitrogen adsorption measurements at 77 K were performed in a home-made high-resolution manometric equipment designed and constructed by the LMA group. CO₂ adsorption/desorption isotherms were performed at 273 K and 298 K using the same equipment and under the same experimental conditions.

Scanning electron microscopy images of as synthesized ZIF-4 were performed using a JEOL JSM-840 microscope.

Synchrotron X-ray powder diffraction data (SXRPD) were collected on the powder-diffraction end station of the MSPD beamline at synchrotron ALBA in Spain, using a MYTHEN detector and a wavelength of 0.4427 Å. The experiments were performed in an *ad hoc* capillary reaction cell (fused silica capillary, inner diameter 0.7 mm, outer diameter 0.85 mm). Before the experiment the ZIF-4 samples were placed inside the capillary connected on-line to a gas-handling and a vacuum line. An Oxford Cryostream 700 was used to control the temperature of the sample. In-situ SXRPD measurements were performed at 298 K and 80 K and varying pressures (vacuum up to 1 bar).

Inelastic neutron scattering (INS) measurements were performed at the VISION beamline (BL-16B) of the Spallation Neutron Source (SNS), Oak Ridge National Laboratory (ORNL), USA. About 200 mg of ZIF-4 was loaded in an Al sample holder connected to a gas handling system. The blank sample was first evacuated for 48h at 413 K and subsequently cooled down to 5 K. Once at this temperature, the INS spectrum was collected for several hours (the background for the instrument and sample holder is negligible in this case since the hydrogenous sample scatters neutrons very strongly). After the background measurement, the ZIF-4 was loaded with N₂ at 80 K up to 103 kPa for a few hours. The dosed sample was cooled down to 5 K and the INS was re-measured for several hours. A similar experiment was performed after dosing CO₂ at 298 K up to 103 kPa, followed by cooling down to 5 K.

Molecular Dynamic Simulations

Molecular Dynamics simulations were performed following the procedure and forcefield that were used previously by one of us to simulate the temperature induced transition in ZIF-7.¹³ We performed a heating procedure consisted of a series of *NpT* simulations with anisotropic barostat at progressively increasing temperature from 10 K to 1510 K. We used 3x2x2 supercell of ZIF-4 converted to P1 symmetry. This heating procedure allows the unit cell vectors and angles to adjust freely in response to temperature. Higher temperatures dramatically increase entropic contributions to the free energy ($F = E - TS$), and facilitate crossing the free energy barriers and transitions to entropically more favorable structures, namely structures with higher pore volume and symmetry.¹³ While this procedure does not guarantee that the all possible polymorphs of the material will be observed in simulations, it is effective for predicting the existence of high volume expanded structures.

Grand Canonical Monte Carlo (GCMC) simulations were performed to load the N₂ molecule, following by the MD simulations in *NpT* ensemble to confirm the stability of the expanded ZIF-4 structure at 77 K. Details are provided in the Supporting Information.

Conclusions

In summary, combination of synchrotron X-ray diffraction and inelastic neutron scattering measurements under operando conditions clearly show that ZIF-4 exhibits a breathing phenomenon upon nitrogen adsorption at ~30 kPa, associated with a 8-9% volume expansion in the unit cell. The transition from a narrow-pore (*np*) to an expanded-pore (*ep*) phase explains the complex behavior of the nitrogen adsorption isotherm at cryogenic temperatures. The existence of an expanded ZIF-4 has been predicted by molecular simulations. First, the expanded ZIF-4 structure was predicted by MD simulations at higher temperatures, which increases entropic contributions to the free energy and stabilizes the expanded structure. Second, the expanded ZIF-4 structure with N₂ molecules was confirmed by MD and GCMC simulations at 77 K. Although CO₂ with a lower kinetic diameter and at a much higher adsorption temperature is able to access in the inner cavities in ZIF-4, this molecule is not able to promote the *np* to *ep* transition at ambient temperature. However, INS measurements show that only at cryogenic temperatures (5 K) CO₂ is able to promote certain structural changes.

Conflicts of interest

There are no conflicts to declare.

Acknowledgements

Authors would like to acknowledge financial support from MINECO (MAT2016-80285-p), Generalitat Valenciana (PROMETEOII/2014/004), H2020 (MSCA-RISE-2016/NanoMed Project), Spanish ALBA synchrotron (Projects AV-2017021985 and IH-2018012591) and Oak Ridge beam time availability (Project IPTS-20843.1). JSA and JGL acknowledge financial support from UA (ACIE17-15) to cover all the expenses for INS measurements at Oak Ridge. JGL acknowledge GV (GRISOLIAP/2016/089) for the research contract. The computing resources were made available through the VirtuES and the ICE-MAN projects, funded by Laboratory Directed Research and Development program at ORNL.

Notes and references

- 1 A. Phan, C.J. Doonan, F.J. Uribe-Romo, C.B. Knobler, M. O'Keeffe, O.M. Yaghi, *Acc. Chem. Res.*, 2010, **43**, 58-67.
- 2 K.S. Park, Z. Ni, A.P. Cote, J.Y. Choi, R. Huang, F.J. Uribe-Romo, H.K. Chae, M. O'Keeffe, O.M. Yaghi, *PNAS*, 2006, **103**, 10186-10191.
- 3 M.R. Ryder, B. Civalleri, T. Bennett, S. Henke, S. Rudic, G. Cinque, F. Fernández-Alonso, J.C. Tan, *Phys. Rev. Lett.*, 2014, **113**, 215502.
- 4 M.E. Casco, Y.Q. Cheng, L.L. Daemen, D. Fairen-Jimenez, E.V. Ramos-Fernández, A.J. Ramirez-Cuesta, J. Silvestre-Albero, *Chem. Commun.*, 2016, **52**, 3639-3642.
- 5 D. Fairén-Jimenez, S.A. Moggach, M.T. Wharmby, P.A. Wright, S. Parsons, T. Düren, *J. Am. Chem. Soc.*, 2011, **133**, 8900-8902.
- 6 M.E. Casco, J. Fernández-Catalá, Y.Q. Cheng, L.L. Daemen, A.J. Ramirez-Cuesta, C. Cuadrado-Collados, J. Silvestre-Albero, E.V. Ramos-Fernández, *ChemistrySelect*, 2017, **2**, 2750-2753.

- 7 S. Aguado, G. Bergeret, M. Pera Titus, V. Moizan, C. Nieto-Dracchi, N. Bats, D. Farrusseng, *New J. Chem.*, 2011, **35**, 546-550.
- 8 C. Cuadrado-Collados, J. Fernández-Català, F. Fauth, Y.Q. Cheng, L.L. Daemen, A.J. Ramirez-Cuesta, J. Silvestre-Albero, *J. Mater. Chem. A*, 2017, **5**, 20938-20946.
- 9 T.D. Bennett, S. Cao, J.-C. Tan, D.A. Keen, E.G. Bithell, P.J. Beldon, T. Friscic, A.K. Cheetham, *J. Am. Chem. Soc.*, 2011, **133**, 14546-14549.
- 10 M. Hartmann, U. Böhme, M. Hovestadt, C. Paula, *Langmuir*, 2015, **31**, 12382-12389.
- 11 M.T. Wharmby, S. Henke, T.D. Bennett, S.R. Bajpe, I. Schwedler, S.P. Thompson, F. Gozzo, P. Simoncic, C. Mellot-Draznieks, H. Tao, Y. Yue, A.K. Cheetham, *Angew. Chem. Int. Ed.*, 2015, **54**, 6447-6451.
- 12 T.D. Bennett, P. Simoncic, S.A. Moggach, F. Gozzo, P. Machi, D.A. Keen, J.-C. Tan, A.K. Cheetham, *Chem. Commun.*, 2011, **47**, 7983-7985.
- 13 Y. Du, B. Wooler, M. Nines, P. Kortunov, S.C. Paur, J. Zengel, S.C. Weston, P.I. Ravikovitch, *J. Am. Chem. Soc.*, 2015, **137**, 13603-13611.
- 14 A.J. Ramirez-Cuesta, *Comptu. Phys. Commun.*, 2004, **157**, 226-228.
- 15 S. Hwang, A. Gopalan, M. Hovestadt, F. Piepenbreier, C. Chmelik, M. Hartmann, R. Snurr, J. Kärger, *Molecules*, 2018, **23**, 668.

View Article Online
DOI: 10.1039/C8TA09713E

Table of Content

View Article Online
DOI: 10.1039/C8TA09713E**Pufferfish effect in ZIF-4:**

Synchrotron powder X-ray diffraction studies under operando conditions confirm that ZIF-4 experience a breathing phenomenon above ~ 30 kPa associated with a large expansion in unit cell volume ($\sim 8\text{-}9\%$). The narrow-pore (np) to expanded-pore (ep) structural transformation is highly sensitive to the nature of the probe molecule and the adsorption temperature. The expanded-pore (N_2) ZIF-4 structure is predicted by molecular simulations.

